Electronic Supplementary Information for

Phosphorus modulation of mesoporous rhodium film for enhanced nitrogen electroreduction

Ziqiang Wang, Wenjing Tian, Hongjie Yu, Tongqing Zhou, Peng Wang, You Xu, Xiaonian Li, Liang Wang and Hongjing Wang*

State Key Laboratory Breeding Base of Green-Chemical Synthesis Technology, College of Chemical Engineering, Zhejiang University of Technology, Hangzhou 310014, P. R. China

Corresponding author

*E-mail: hjw@zjut.edu.cn

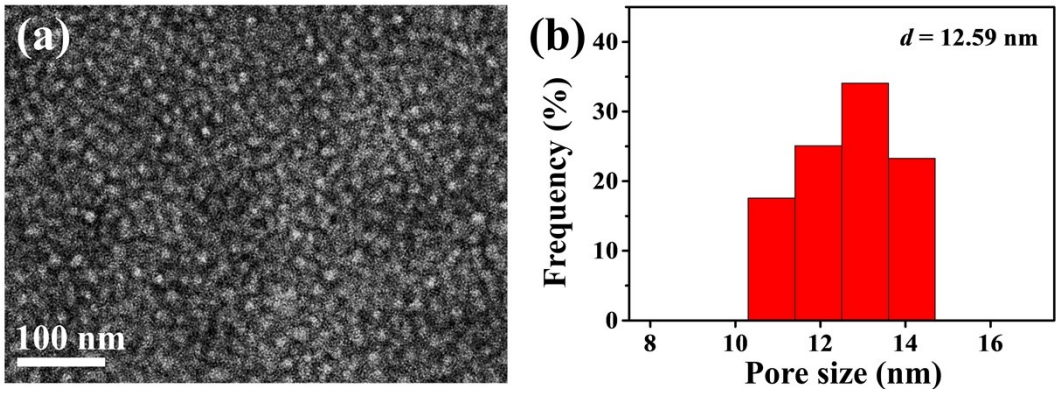

Fig. S1 TEM image and corresponding pore size distribution of the P-mRh/NF.

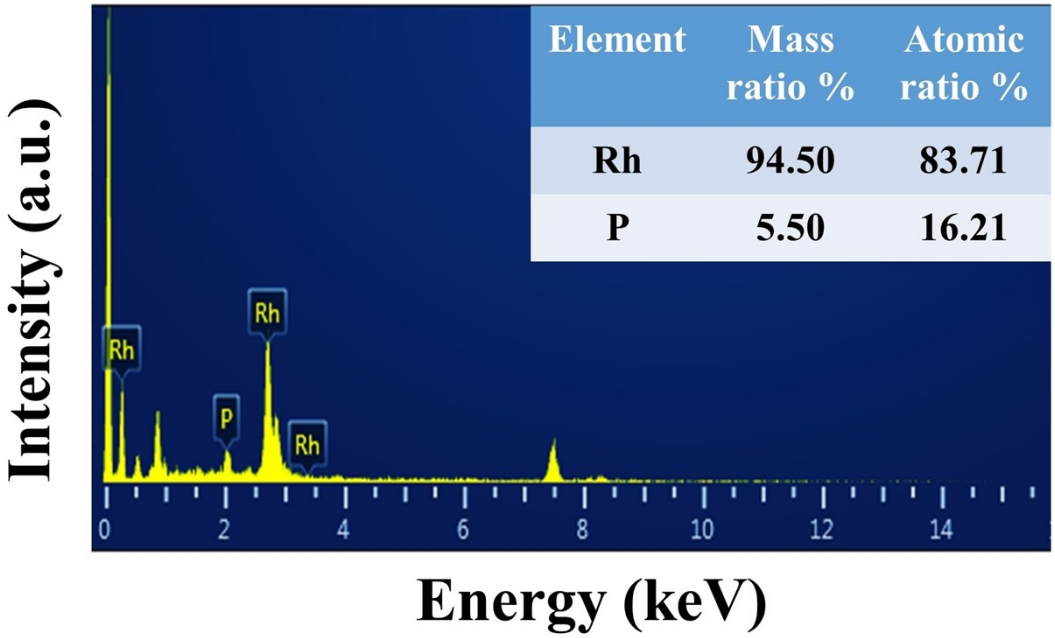

Fig. S2 EDX spectrum of the P-mRh film and corresponding element amount.

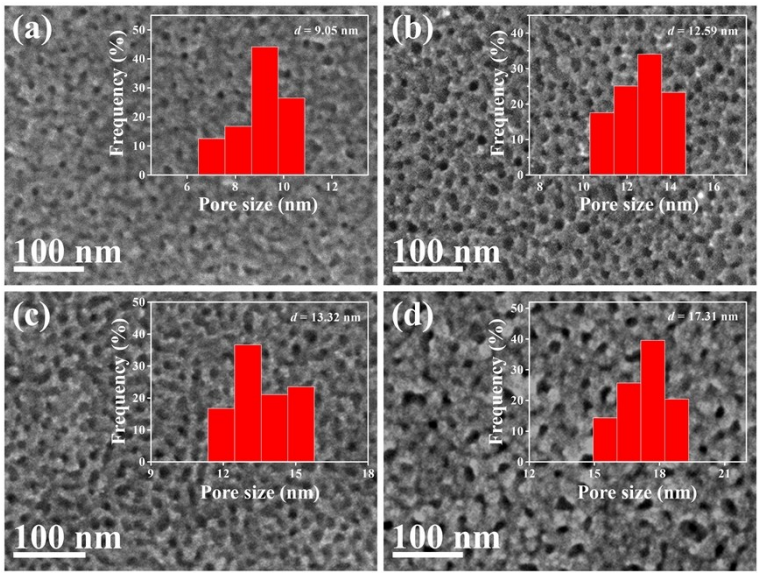

Fig. S3 SEM images and corresponding pore size distribution of P-mRh/NF obtained in different amount of THF: (a) 0.25 mL, (b) 0.5 mL, (b) 1.0 mL, and (d) 1.5 mL.

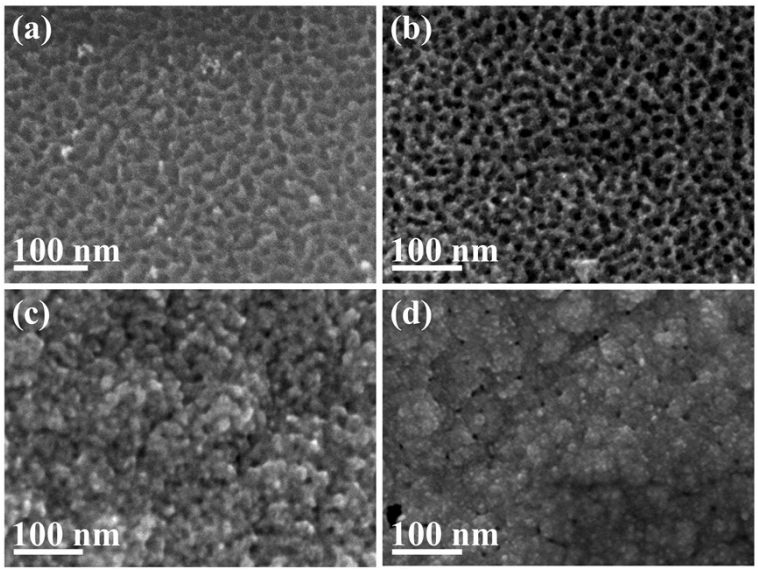

Fig. S4 SEM images of P-mRh/NF obtained by electrodeposition of different molar concentrations of sodium hypophosphite solution: (a) 0 mM, (b) 2.5 mM, (b) 10 mM, and (d) 20 mM.

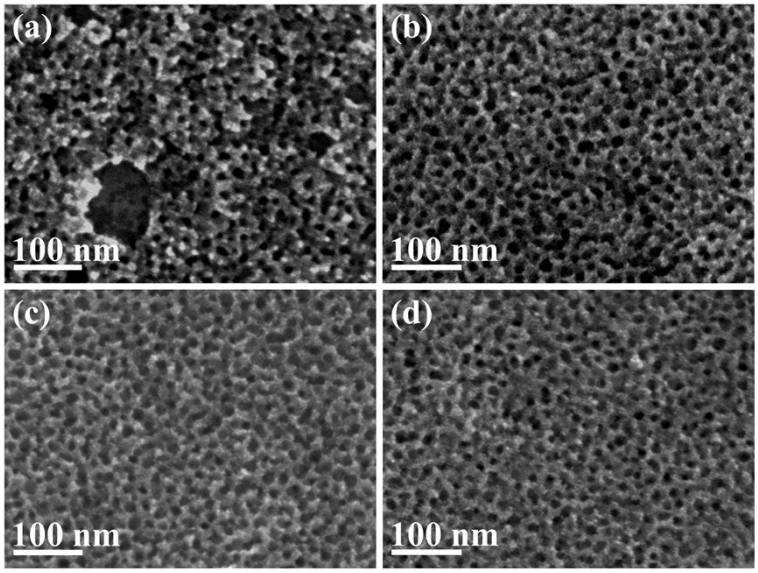

Fig. S5 SEM images of typical samples at different electrodeposition times for (a) 500 s, (b) 1000 s, (c) 2000 s, and (d) 4000 s.

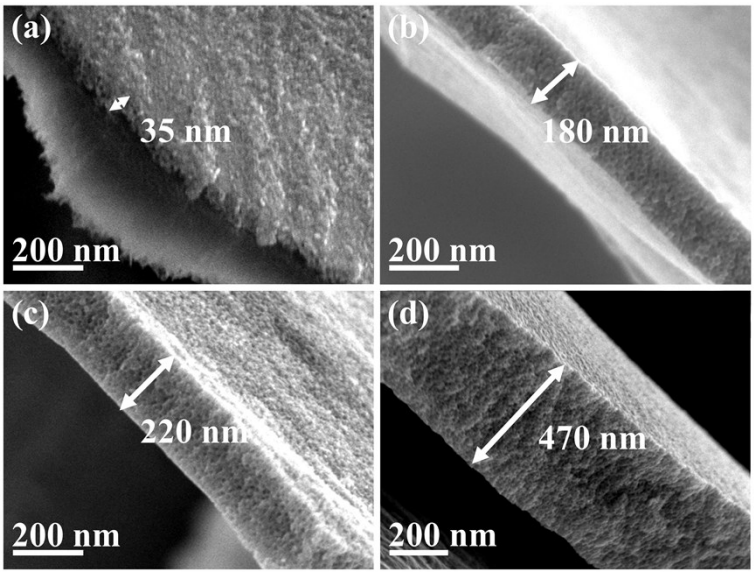

Fig. S6 SEM images of cross-sections of typical samples at different electrodeposition times for (a) 500 s, (b) 1000 s, (c) 2000 s, and (d) 4000 s.

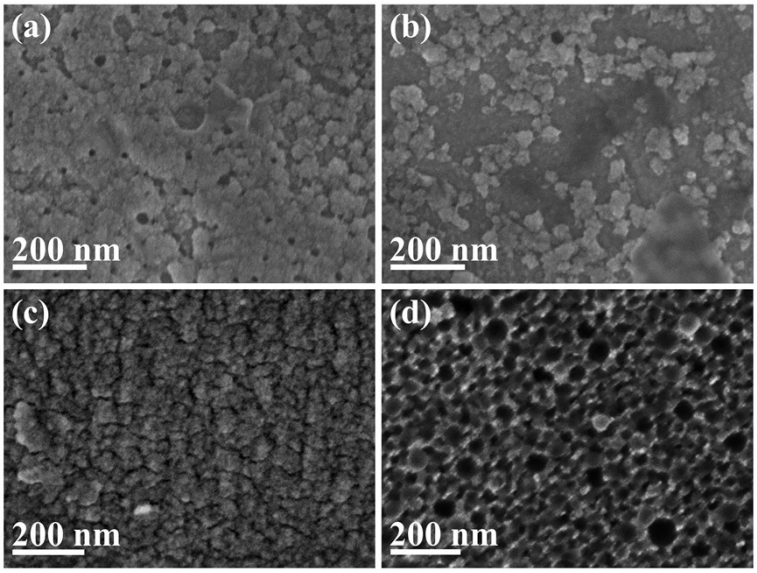

Fig. S7 SEM images of the P-mRh/NF prepared by changing surfactant with (a) F127, (b) Briji 58, (c) DM970, and (d) PS-*b*-PEO.

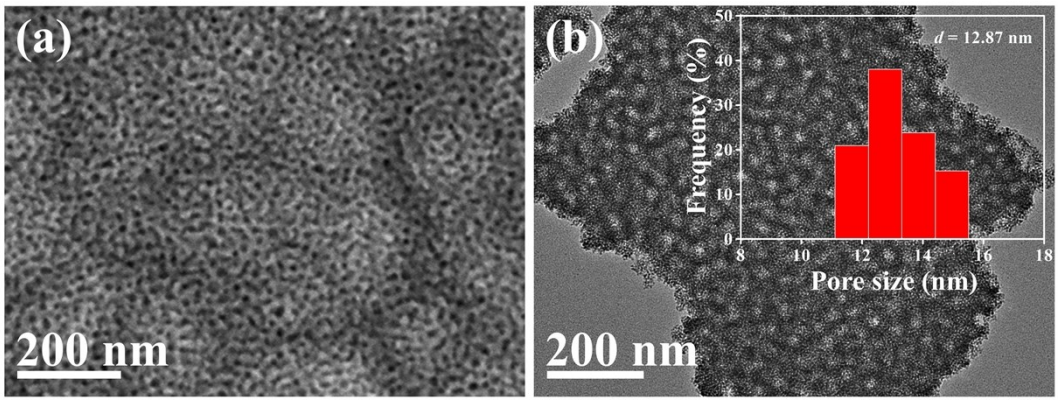

Fig. S8 (a) SEM image of P-mRh/CP. (b) TEM image and corresponding pore size distribution of the P-mRh film.

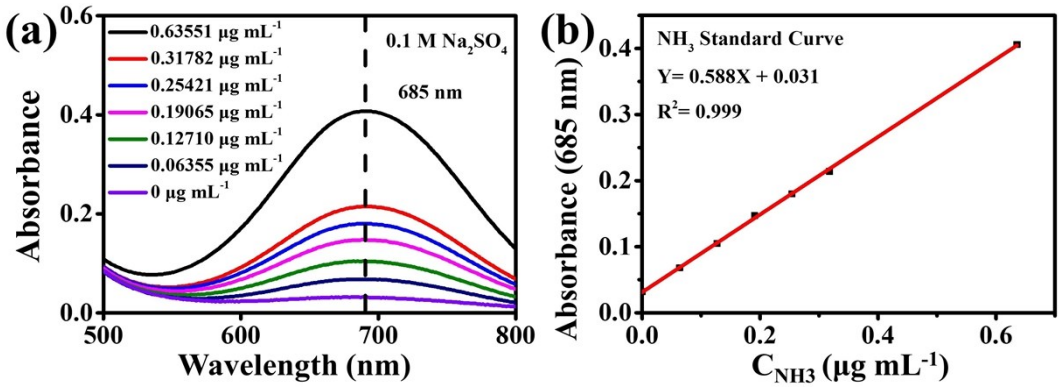

Fig. S9 (a) UV−vis absorption spectroscopy of various NH_4^+ concentrations with the color reagent for 1 h at room temperature. (b) Calibration curve used to estimate the concentrations of NH_3.

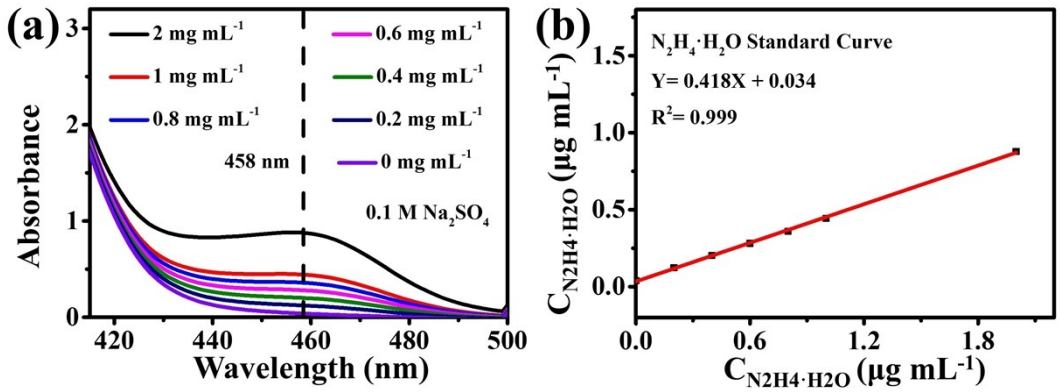

Fig. S10 (a) UV-Vis curves of different concentrations of hydration solution were measured after incubated for 15 min at 25 °C. (b) Calibration curve used for estimation of $N_2H_4 \cdot H_2O$ concentration.

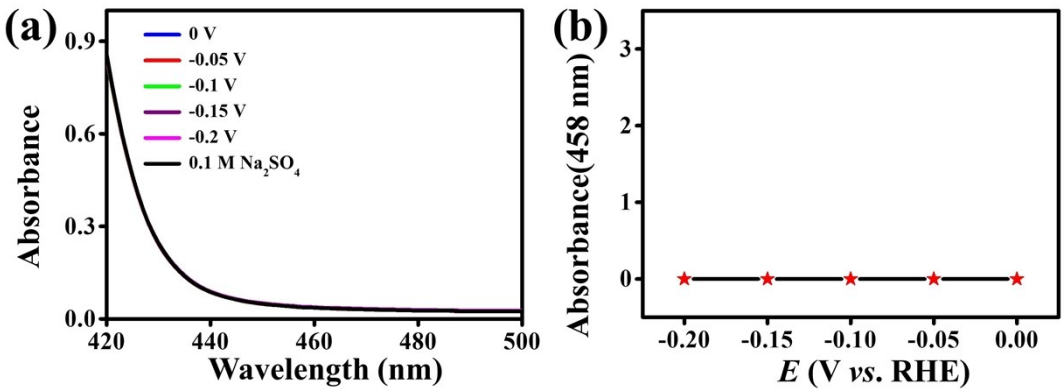

Fig. S11 UV-vis spectra of the electrolytes after 2h electrolysis in nitrogen at different potentials and (b) the $N_2H_4 \cdot H_2O$ concentration of the electrolyte.

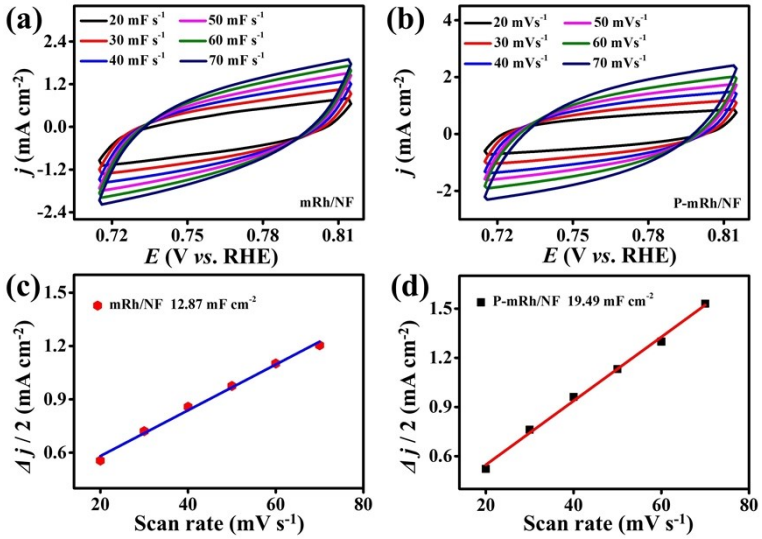

Fig. S12 CV curves of mRh/NF (a) and P-mRh/NF (b) in the range of 0.08 and 0.18 V. Capacitive current densities derived from CVs at 0.765 V against scan rates for mRh/NF (c) and P-mRh/NF (d).

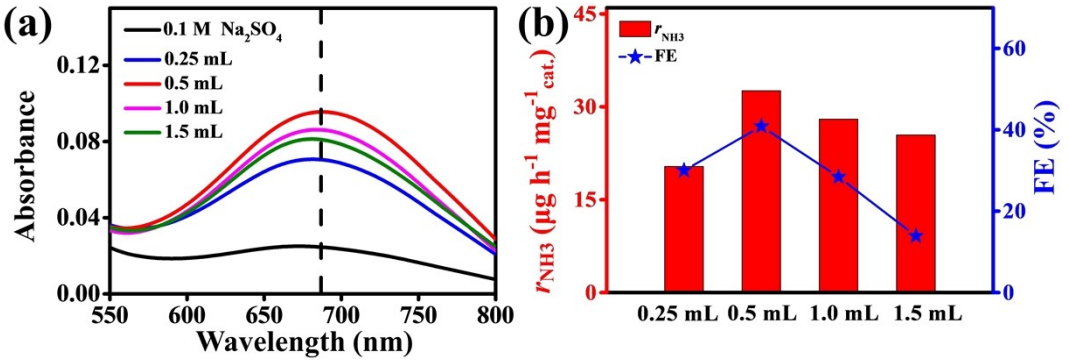

Fig. S13 (a) UV-Vis absorption spectra of P-mRh/NF obtained from different amounts of THF and (b) corresponding FE and r_{NH3}.

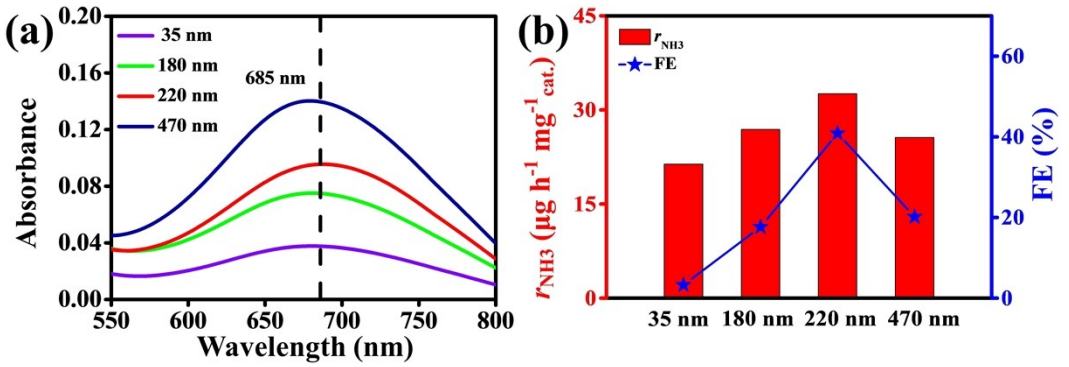

Fig. S14 (a) UV-Vis absorption spectra of samples with different thickness and (b) corresponding Faraday efficiencies and NH_3 yields.

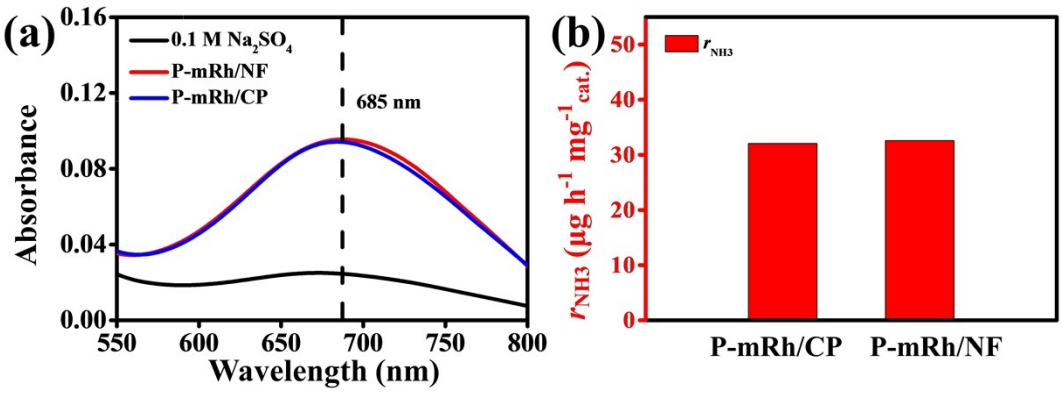

Fig. S15 UV-Vis absorption spectra of P-mRh/NF and P-mRh/CP and (b) corresponding r_{NH3}.

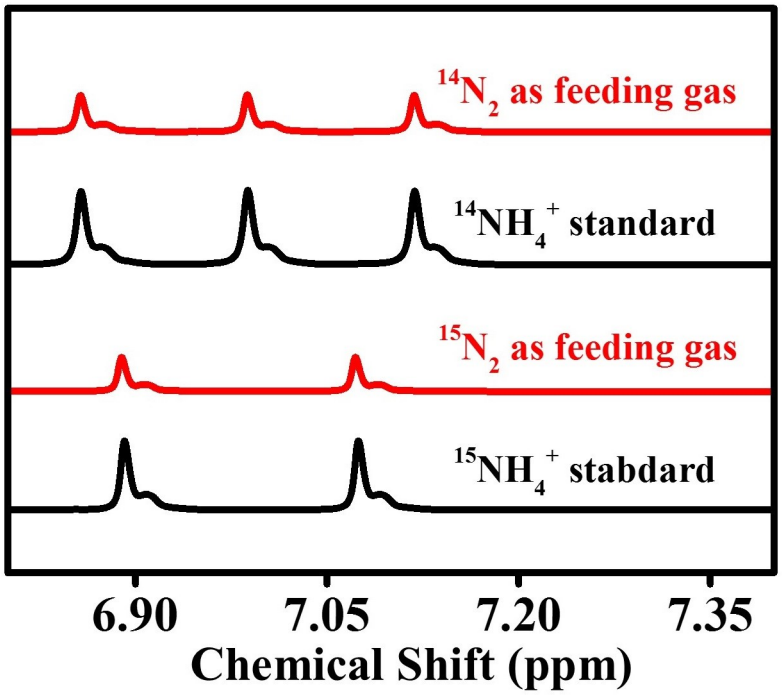

Fig. S16 ^{1}H-NMR spectra of standard $^{14}NH_4^+$, $^{15}NH_4^+$ solution, and the electrolytes produced from the NRR reaction using $^{14}N_2$ and $^{15}N_2$ as the N_2 source.

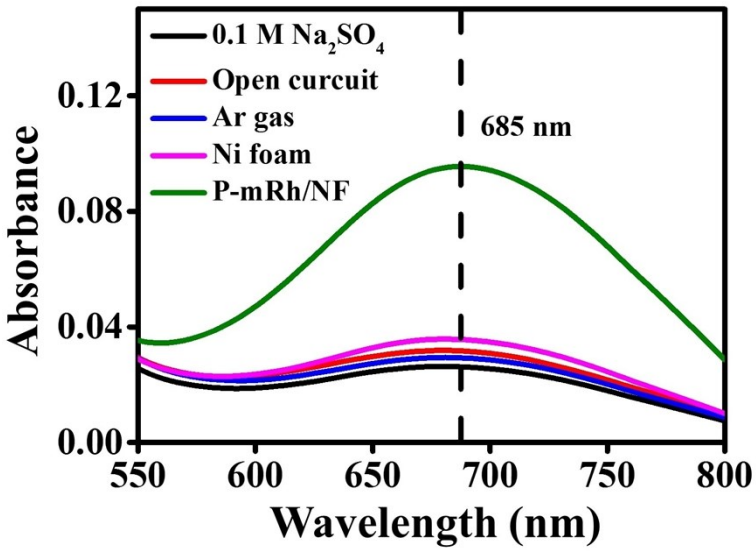

Fig. S17 UV-vis absorption spectra of the electrolytes under different conditions.

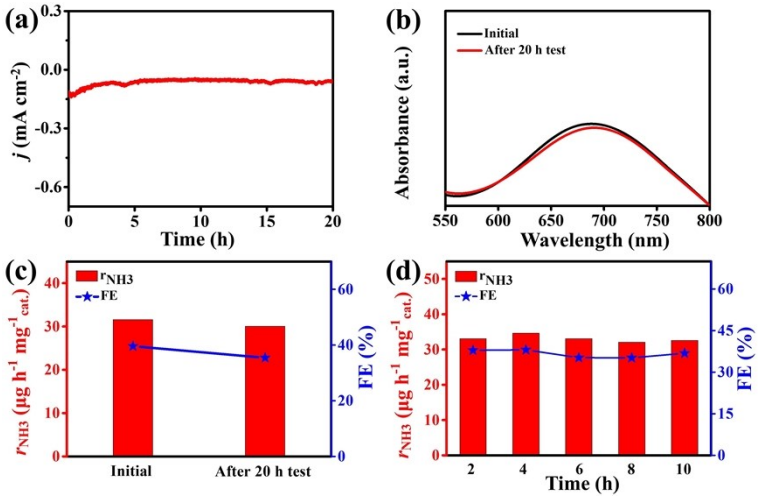

Fig. S18 (a) Chronocurrent curves of typical potentials for 20 h. (b) UV−vis absorption spectras of the electrolytes before and after the durability tests and (c) their NH_3 yield and FE. (d) The NH_3 yields and corresponding FE after five cycle measurements.

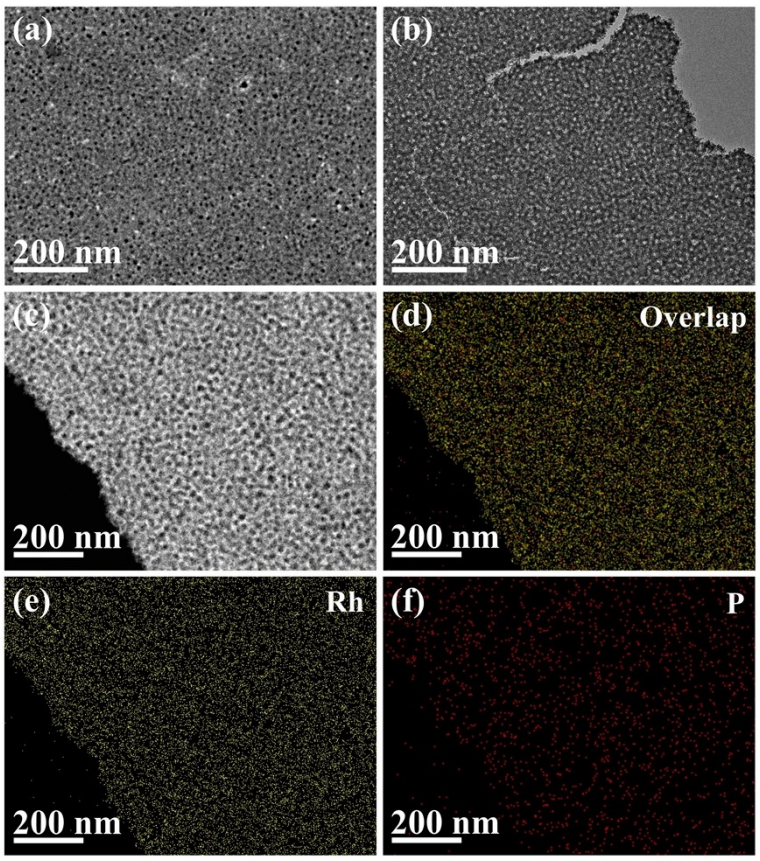

Fig. S19 Characterization of the morphology and compositition of the P-mRh/NF after the durability test. (a) SEM image of of the P-mRh/NF, and (b) TEM iamge, (c) HAADF-STEM and (d-f) corresponding EDX elemental mapping images of the P-mRh film.

Table S1 The mass percentage of P in the P-mRh/NF obtained from different molar concentrations of sodium hypophosphite solution.

Samples	Phosphorus percentage (wt%)
$P_{2.5}$-mRh/NF	2.99
P_{10}-mRh/NF	9.62
P_{20}-mRh/NF	13.03

Table S2 The comparisons of the NRR performance of the P-mRh/NF with the representative reported catalysts under ambient conditions.

Catalyst	Electrolyte	NH_3 yield	FE (%)	Ref.
P-mRh/NF	**0.1 M Na_2SO_4**	**32.57 μg h^{-1} $mg^{-1}_{cat.}$**	**40.86**	**This work**
Ag film	0.1 M Na_2SO_4	1.27 μg h^{-1} cm^{-2}	7.36	1
mAu_3Pd/NF	0.1 M Na_2SO_4	24.02 μg h^{-1} $mg^{-1}_{cat.}$	18.16	2
Porous Au Film	0.1 M Na_2SO_4	9.42 μg h^{-1} cm^{-2}	13.36	3
PdCuIr-LS	0.1 M Na_2SO_4	113.43 μg h^{-1} $mg^{-1}_{cat.}$	1.84	4
MoS_2 nanoflower	0.1 M Na_2SO_4	29.28 μg h^{-1} $mg^{-1}_{cat.}$	8.34	5
NiO/G	0.1 M Na_2SO_4	18.6 μg h^{-1} $mg^{-1}_{cat.}$	7.8	6
Mo_2N nanorods	0.1 M HCl	78.4 μg h^{-1} $mg^{-1}_{cat.}$	4.5	7
dendritic Cu	0.1 M HCl	25.63 μg h^{-1} $mg^{-1}_{cat.}$	15.12	8
Bi nanodendrites	0.1 M HCl	25.86 μg h^{-1} $mg^{-1}_{cat.}$	10.8	9
Au/Bi NSs	0.1 M HCl	20.39 μg h^{-1} mg^{-1}_{cat}	15.53	10

References

1. L. Ji, X. Shi, A. M. Asiri, B. Zheng and X. Sun, *Inorg. Chem.*, 2018, **57**, 14692-14697.
2. H. Yu, Z. Wang, S. Yin, C. Li, Y. Xu, X. Li, L. Wang and H. Wang, *ACS Appl. Mater. Interfaces*, 2020, **12**, 436-442.
3. H. Wang, H. Yu, Z. Wang, Y. Li, Y. Xu, X. Li, H. Xue and L. Wang, *Small*, 2019, **15**, 1804769.
4. R. D. Kumar, Z. Wang, C. Li, A. V. N. Kumar, H. Xue, Y. Xu, X. Li, L. Wang and H. Wang, *J. Mater. Chem. A*, 2019, **7**, 3190-3196.
5. X. Li, T. Li, Y. Ma, Q. Wei, W. Qiu, H. Guo, X. Shi, P. Zhang, A. M. Asiri, L. Chen, B. Tang and X. Sun, *Adv. Engergy Mater.*, 2018, 8, 1801357.
6. K. Chu, Y.-p. Liu, J. Wang and H. Zhang, *ACS Appl. Energy Mater.*, 2019, **2**, 2288-2295.
7. X. Ren, G. Cui, L. Chen, F. Xie, Q. Wei, Z. Tian and X. Sun, *Chem. Commun.*, 2018, **54**, 8474-8477.
8. C. Li, S. Mou, X. Zhu, F. Wang, Y. Wang, Y. Qiao, X. Shi, Y. Luo, B. Zheng, Q. Li and X. Sun, *Chem. Commun.*, 2019, **55**, 14474-14477.
9. F. Wang, X. Lv, X. Zhu, J. Du, S. Lu, A. A. Alshehri, K. A. Alzahrani, B. Zheng and X. Sun, *Chem. Commun.*, 2020, **56**, 2107-2110.
10. Y. Xu, T. Ren, S. Yu, K. Ren, M. Wang, Z. Wang, X. Li, L. Wang and H. Wang, *Sustainable Energy Fuels*, 2020, **4**, 4516-4521.